Proceedings of ASME Turbo Expo 2011
GT2011
June 6-10, 2011, Vancouver, British Columbia, Canada

GT2011-45205

CONTRA-ROTATING OPEN ROTOR OPERATION FOR IMPROVED AERODYNAMICS AND NOISE AT TAKEOFF

Alexios Zachariadis, Cesare A. Hall[1]
Whittle Laboratory
University of Cambridge
United Kingdom

Anthony B. Parry
Rolls-Royce plc
Derby
United Kingdom

ABSTRACT

The contra-rotating open rotor is, once again, being considered as an alternative to the advanced turbofan to address the growing pressure to cut aviation fuel consumption and carbon dioxide emissions. One of the key challenges is meeting community noise targets at takeoff. Previous open rotor designs are subject to poor efficiency at takeoff due to the presence of large regions of separated flow on the blades as a result of the high incidence needed to achieve the required thrust. This is a consequence of the fixed rotor rotational speed constraint typical of variable pitch propellers.

Within the study described in this paper, an improved operation is proposed to improve performance and reduce rotor-rotor interaction noise at takeoff. Three-dimensional computational fluid dynamics (CFD) calculations have been performed on an open rotor rig at a range of takeoff operating conditions. These have been complemented by analytical tone noise predictions to quantify the noise benefits of the approach.

The results presented show that for a given thrust, a combination of reduced rotor pitch and increased rotor rotational speed can be used to reduce the incidence onto the front rotor blades. This is shown to eliminate regions of flow separation, reduce the front rotor tip loss and reduce the downstream stream tube contraction. The wakes from the front rotor are also made wider with lower velocity defect, which is found to lead to reduced interaction tone noise. Unfortunately, the necessary increase in blade speed leads to higher relative Mach numbers, which can increase rotor alone noise.

In summary, the combined CFD and aero-acoustic analysis in this paper shows how careful operation of an open rotor at takeoff, with moderate levels of re-pitch and speed increase, can lead to improved front rotor efficiency as well as appreciably lower overall noise across all directivities.

[1] Corresponding author, e-mail address: cah1003@cam.ac.uk

NOMENCLATURE

B	Blade Number
$C_P = \dfrac{p - p_\infty}{p_{0\infty} - p_\infty}$	Pressure Coefficient
D	Rotor Diameter [m]
$exp(-s/R)$	Entropy Function
g	Axial Gap Between Rotors [m]
M	Mach Number
N	Rotor Rotational Speed [rad. s^{-1}]
p, p_0	Static, Stagnation Pressure [Pa]
Q	Torque [N.m]
r	Radius [m]
R	Tip Radius [m], Gas Constant [J. $kg^{-1}.K^{-1}$]
s	Entropy [J.$kg^{-1}.K^{-1}$], Rotor Pitch [m]
T	Thrust [N]
U	Blade Speed [m.s^{-1}]
V	Velocity [m.s^{-1}]
W	Relative Velocity [m.s^{-1}]
x	Axial Distance [m]
$Y_P = \dfrac{p_{02,rel} - p_{01,rel}}{p_{01,rel} - p_1}$	Loss Coefficient
β	Relative Flow Angle [rad]
$\eta_{prop} = \dfrac{TV_\infty}{QN}$	Propeller Efficiency
θ	Pitchwise Location [m]

Subscripts

F, R	Front, Rear Rotor
∞	Freestream
is	Isentropic
rel	Relative
tip	Rotor Tip
1, 2	Upstream, Downstream of Rotor

INTRODUCTION

The increasing pressure for fuel efficiency and minimal environmental impact is encouraging aircraft operators to adopt new technologies. In parallel to the evolution of turbofan engines, alternative solutions are being developed which provide a step change in efficiency. Open rotor engines have the potential to deliver double-digit fuel savings compared to turbofan engines of equivalent thrust [1]. A contra-rotating propeller system creates minimal residual swirl downstream of the engine, which leads to higher propulsive efficiency than a single rotor propeller [2]. In addition, unlike conventional turboprop engines, the open rotor is capable of operating efficiently at a cruise Mach number similar to turbofan-powered aircraft.

One of the aerodynamic challenges facing the open rotor is the need to achieve good performance and low-noise at takeoff whilst maintaining high efficiency at cruise. Contrary to a ducted turbofan engine, the flow conditions presented to the open rotor blades vary considerably for different points in the flight envelope. In particular, the absence of a nacelle means that the axial Mach number just upstream of the rotors is much lower at takeoff than at cruise. Since propeller engines are typically operated at constant rotational speed this leads to large variations in the inlet relative flow angles and a blade pitch change mechanism is needed in order to control the blade incidence whilst achieving the aircraft thrust requirements.

A number of studies such as Mitchell [3] have been published regarding the aerodynamic performance of open rotors at a range of Mach numbers. Detailed experimental flow-field investigations are however more scarce, and include the works of Neumann *et al.* [4] for single-rotation rotors, and Podboy and Krupar [5] and Shin *et al.* [6] for contra-rotation. These investigations constituted the major source of understanding of advanced propeller flows with various Euler computational studies being performed alongside [7]. Recently, with the advent of modern Navier-Stokes solvers and the renewed interest in open rotor configurations, 3D steady and unsteady simulations are becoming routine. In Schnell *et al.* [8] and Peters and Spakovszky [9], results from advanced CFD are combined with aeroacoustic methods in order to assess the noise sources and optimise the open rotor designs. Studies such as these have shown that various design modifications combined with changes in operating conditions have the potential to improve performance and reduce noise. However, there have been no detailed investigations into the effects of varying the open rotor operating conditions independently of any design changes.

In this paper, a simple open rotor configuration is chosen that has been studied extensively and used previously for validating the CFD approach [10]. The flow-field at takeoff is examined and the features that lead to poor performance and noise are addressed by gradually changing the open rotor operating condition. Only the rotational speed and blade setting angles are varied, whilst maintaining a constant net thrust. It is shown that adjusting the open rotor operation in this way can reduce the loss sources and create a cleaner, more two-dimensional flow-field. A noise prediction tool is then applied to explore how the changes in the flow-field translate into differences in the radiated noise.

This paper aims to explain how modifying the operating conditions of an open rotor can control the flow features that lead to high loss and unsteady interaction. It demonstrates that speeding up and re-pitching the front rotor is an effective way of improving the aerodynamics and noise at takeoff.

OPEN ROTOR TEST CASE

The test case for this paper is the Rolls-Royce Rig-140 contra-rotating open rotor model engine fitted with straight blades. Details of the rig and experimental methods are described by Kirker [11]. The key parameters for the configuration are given in Table 1. This includes the blade setting angles (measured from the tangential direction) for the nominal takeoff and cruise conditions.

Geometry Parameters	**Value**	
Rotor Diameter (D) [m]	0.76	
Hub:Tip Ratio	0.32	
Rotor-Rotor Axial Spacing (g/D)	0.21	
Performance Parameters	**Cruise**	**Take-Off**
Flight Mach Number (M_∞)	0.75	0.20
Front Blade Angle at r/R=0.7 [deg]	68.00	48.10
Rear Blade Angle at r/R=0.7 [deg]	62.52	42.39

Table 1. Rig-140 key parameters.

The rotor blade used in this paper is illustrated in Fig. 1 and its geometrical characteristics are presented in Fig. 2. The geometry is the same for both front and rear rotors. This blade was selected because it is the simplest high-speed geometry available, test data is available for its performance and it has already been studied extensively to validate the CFD approach applied in this paper, see [10]. A simple high-speed geometry was preferred so that the effects of rotor operation could be separated from the effects of rotor design features. The applicability of the study to more advanced swept blades is discussed in a later section.

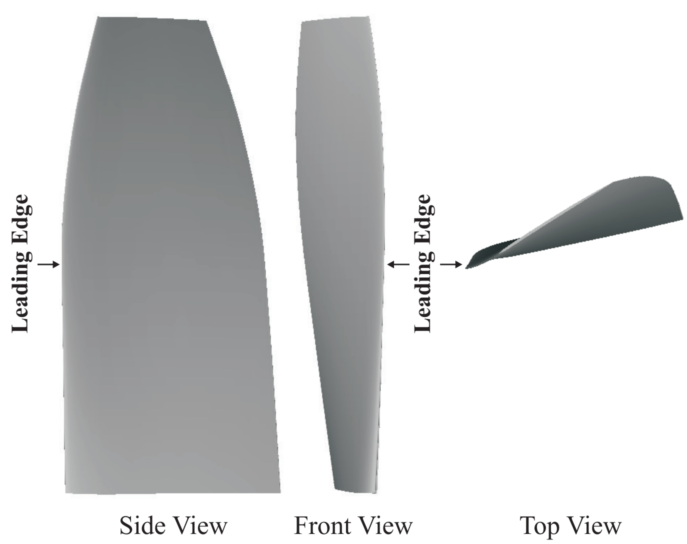

Fig. 1. Overview of the Rig-140 straight blade geometry.

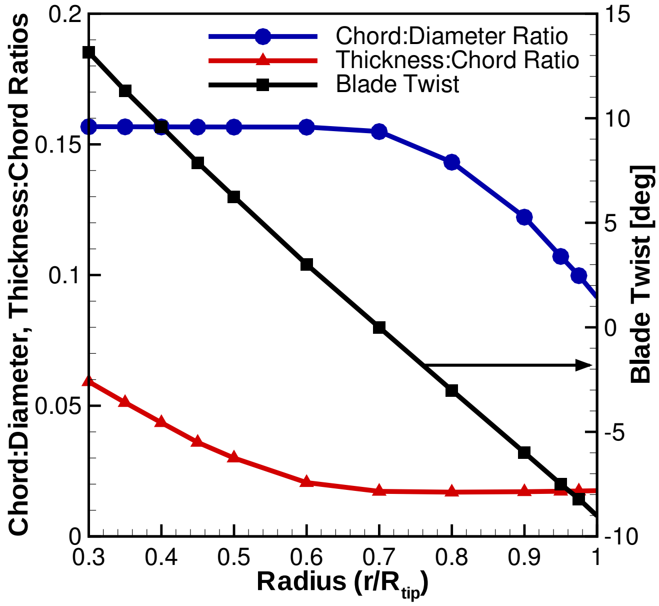

Fig. 2. Summary of blade geometrical characteristics.

COMPUTATIONAL METHODS

All CFD computations presented in this paper have been run using HYDRA [12] with the Spalart-Allmaras one-equation turbulence model [13]. For all details pertaining to the computational domain, meshing, boundary conditions and calculation set-up see Zachariadis and Hall [10]. Only fully converged steady calculation results are used in this paper.

As detailed in [10] the CFD approach applied has been shown to be accurate for predicting open rotor performance. Various flow-field measurements have also been well reproduced. Two examples of comparison between rig data and computational results are shown in Figs. 3 and 4, for takeoff and cruise at the nominal operating conditions given in Table 1.

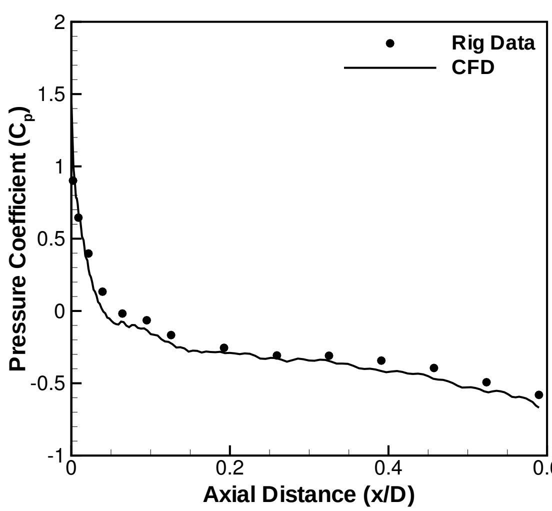

Fig. 3. Experimental and calculated distributions of pressure coefficient (C_P) on the rig bullet surface at takeoff, from [10].

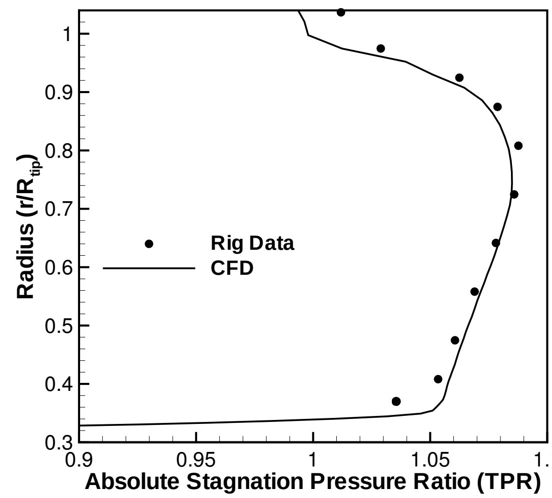

Fig 4. Measured and calculated cruise absolute stagnation pressure ratio (*TPR*) downstream of the contra-rotating rotors at cruise.

The noise calculations presented in this paper were completed using the method detailed in [14], known as CRPFAN. This code has been shown to give close agreement with measured noise data for uninstalled contra-rotating open rotor configurations at both low and high speed flight conditions [15]. In CRPFAN, the steady loading and thickness noise of each rotor is computed in the frequency-domain using a non-compact source model. Each rotor is treated as an independent source, with a fixed axial distance between the rotor pitch change axes. The acoustic model is based on the work of Hanson [16] who defined a space-fixed, locally orthogonal coordinate system, tied to the helicoidal surface swept by the blade pitch change axis (PCA) as the blade rotates and advances. The advantage of this coordinate system lies in the ease with which conventional aerofoil coordinates can be input into the numerical scheme.

The use of a non-compact source prediction procedure requires knowledge of both spanwise and chordwise distributions of blade loading and thickness. In the model, the spanwise thickness and loading distributions are dependent on the geometry and distribution of lift coefficient respectively which are input. The loading at each spanwise section of the rotor is then decomposed into thrust and torque components using velocity triangles. In the chordwise direction, distributions are specified in the frequency domain. These distributions are Fourier transforms of the chordwise normalised thickness and loading distributions respectively and standard distributions are available in the code.

The calculation of the unsteady loading noise generated by the interaction of the rear rotor with the viscous wakes and tip vortices shed by the front rotor is performed using a chordwise compact acoustic model (in contrast to the steady loading and thickness acoustic model). The unsteady flow-field between the rotors is established using a compressor wake model [17] and a tip vortex model developed at NASA [18]. Spanwise phasing effects, resulting from rotor sweep and lean and the mean flow direction are preserved in this treatment.

The fluctuating lift forces on the rear rotor caused by the upwash from the front rotor wake are computed using the classical unsteady lift response theory of Sears [19] modified to take compressibility effects into account according to a procedure developed by Amiet [20]. The theory is applied at each spanwise section on the rear rotor following a Fourier decomposition of the components of the fluctuating velocity normal to the rear rotor chord. Only these transverse gusts are considered in the calculation. One of the pitfalls of simple methods such as CRPFAN is that the blade rows are treated as compact sources where the lift fluctuation is treated as an acoustic dipole. This procedure is only accurate at low frequency where the acoustic wavelengths are long compared to the chord [21]. The authors note that analytic methods have been developed for, and applied to, the prediction of non-compact acoustic sources on open rotors due to aerodynamic rotor-rotor interaction (see, for example, Parry & Crighton [22] and Parry [23]). However, the associated prediction code is not available in the public domain.

Figure 5 compares the front rotor-alone noise directivities at blade passing frequency as measured on the rig and as predicted by CRPFAN at takeoff conditions. The inflow rig data is given at two locations in the wind tunnel and was acquired by means of a linear traverse at a constant distance away from the rig centreline. At 0.63 diameters, the noise levels are not satisfactorily predicted. Rotor-alone tones are strongly affected by very near-field effects as these depend on the local flow aerodynamics particularly near the blade tip. Considering that no detailed flow information is supplied to CRPFAN, the underprediction of the tone in the very near-field is not surprising. The moderate near-field predictions however, are in much better agreement with measurements.

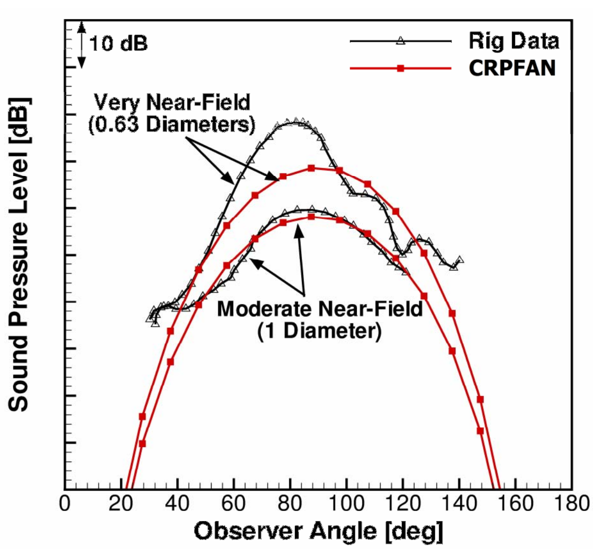

Fig. 5. Comparison of the front rotor-alone noise directivities at blade passing frequency in the very near- and moderate near-field at takeoff.

Measured very near-field noise directivity for the (2,1) rotor-rotor interaction tone at takeoff is compared to predictions in Fig. 6. A comparison for another, but similar, blade design is also presented for the (1,2) interaction tone. The (2,1) interaction tone shows a plateau of maximum noise near the planes of rotor rotation. CRPFAN predicts the directivity well but some discrepancies exist in terms of absolute noise levels between observer angles of 40 to 65° and between 100 to 130°. The agreement between experiments and predictions is good, given the importance of near-field effects and the inability of the CRPFAN code to predict these near-field effects accurately [15]. However, perhaps the accuracy of the predictions for interaction tones is not too surprising as near-field effects tend to be much smaller for interaction tones and, in any case, reduce with increasing frequency.

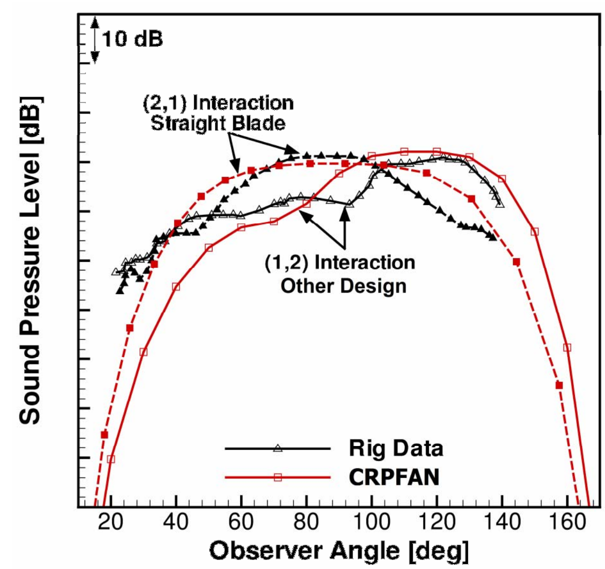

Fig. 6. Very near-field noise directivities of the (2,1) rotor-rotor interaction tone for straight blades at takeoff and (1,2) interaction tone for another blade design at a takeoff condition

AERODYNAMICS AT TAKEOFF CONDITIONS

The blades of an open rotor are re-pitched at takeoff to meet thrust requirements. To generate high thrust, the blades are set at high incidence to the oncoming flow. Figure 7 shows the distribution of incidence along the radius of the rotors for the Rig-140 configuration at the nominal takeoff condition.

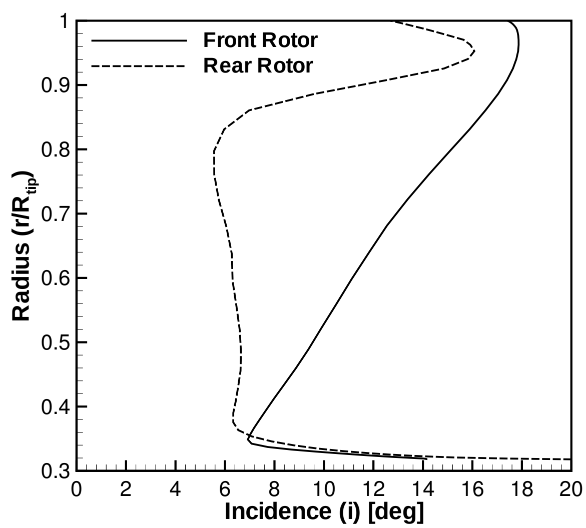

Fig. 7. Radial distribution of the front and rear rotor incidence at the nominal takeoff condition.

At the hub, the front rotor has an incidence of around 7°, which increases linearly towards the tip as a result of the blade twist distribution (Fig. 2). For this operating point, the highest incidence on the front rotor is just below the tip, with a magnitude of 18°. The rear rotor sees much lower incidence along most of its span. It is only near the tip that the incidence is high, which as shown below, is due to interaction with the front rotor tip flow.

Figure 8 gives an overview of the predicted wakes and tip vortex structures at the nominal takeoff condition. The figure illustrates how the high incidence on the front rotor leads to a highly three-dimensional flow-field. The flow separates at the front rotor leading edge in a similar way to the flow over delta wings, as described in [24]. This separated flow rolls-up and reattaches further along the rotor chord, creating a large recirculation zone referred to as a leading edge vortex (LEV), which is convected towards the blade tip. The LEV initates at 55 percent non-dimensional radius, where the section operates at 11° of incidence. The large loss core shown in Fig. 8 downstream of the front rotor is the combined result of the LEV and tip vortex. This tip flow is the dominant source of losses for the front rotor at takeoff and has a significant tangential and radial extent.

The rear rotor generates a smaller LEV and tip vortex because it is operated at lower incidence. However, the flow-field at the tip of the rear rotor is dominated by the interaction with the flow from the front rotor. Across the mixing plane used in the computation, the front blade loss core is circumferentially averaged and forms a “loss ring”. Due to streamtube contraction, the convected ring impinges on the rear rotor and interacts with its tip flow resulting in additional loss. In reality, this interaction is highly unsteady since the loss ring is a number of distinct loss cores from the front rotor rotating in the opposite direction to the tip vortices shed by the rear rotor.

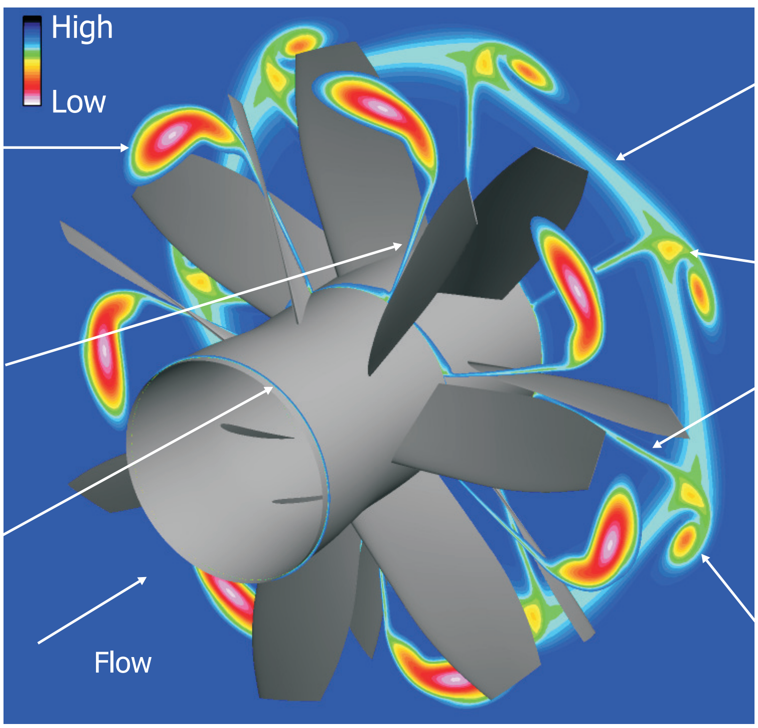

Fig. 8. Contours of entropy function (*exp-(s/R)*) for Rig-140 at the nominal takeoff condition.

IMPROVING THE FRONT ROTOR AERODYNAMICS

To improve the aerodynamics at takeoff, the front rotor incidence must be reduced. The simplest and most effective way to do this is to reduce the blade pitch angle (“Re-Pitch”) but this reduces the blade lift and therefore thrust. To recover the thrust back to nominal levels, the rotor speed can be increased. This section shows that, by combining re-pitch with increased rotational speed, thrust can be maintained and at the same time better aerodynamics achieved.

Figure 9 illustrates the concept of re-pitching and speeding up the front rotor. The velocity triangle at the rotor inlet for the nominal condition at takeoff is shown by the solid lines with a typical pitch angle setting. At this condition, the incidence is high leading to the separated flow shown in Fig. 8. The dashed lines illustrate the effect of an improved rotor operation at the same free-stream velocity. The blade is re-pitched by 20° (“Re-Pitch -20°”) relative to the nominal condition, and the blade speed is increased to recover the lost thrust.

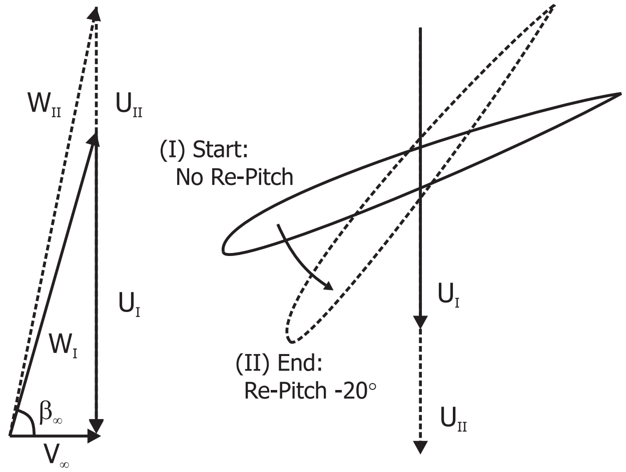

Fig. 9. Rotor face velocity triangles before and after re-pitching and speeding up at takeoff.

To assess the potential of re-pitching and speeding up the front rotor at takeoff, exchange rates were established. A number of HYDRA steady calculations were performed on Rig-140 where the front rotor pitch and speed were varied independently of each other starting from the nominal takeoff condition. These were used to establish the impact of rotor pitch and speed on thrust production and propeller efficiency. The rear rotor was removed from these calculations and new meshes were generated for each re-pitch case. All calculations were run with identical boundary conditions. For cases where the front rotor was re-pitched, the CFD calculations were run without modifying the rotor speed and all other parameters were kept constant. For the cases with rotor speed increases, the rotor pitch was fixed at the nominal value.

The exchange rates are illustrated in Fig. 10 and demonstrate how sensitive the rotor thrust and propeller efficiency are to rotational speed and pitch setting. Increasing rotational speed for a given pitch is effective at increasing thrust with only a small increase in rotor incidence (Fig. 10(a)). Reducing pitch angle for a given rotor speed, on the other hand, reduces thrust much more gradually with incidence. Based on the rate of change of thrust with respect to incidence, these results show that for Rig-140 at takeoff the rotor speed is 7 times as effective as pitch for varying the thrust. Note that this result is specific to the particular configuration. However, it is expected that for all rotor designs thrust will vary more with rotational speed than with pitch since the lift on an aerofoil tends to be proportional to speed squared and only linearly related to incidence.

The propeller efficiency plotted in Fig. 10(b) shows that increasing the rotor tip speed reduces the propeller efficiency. This is a result of lower lift-to-drag ratios at higher incidence. In contrast, re-pitching the blade from the nominal condition reduces the incidence to values at which the rotor operates more efficiently. A peak is visible for the "Re-Pitch -16°" case at which point the rotor incidence is 3.4°.

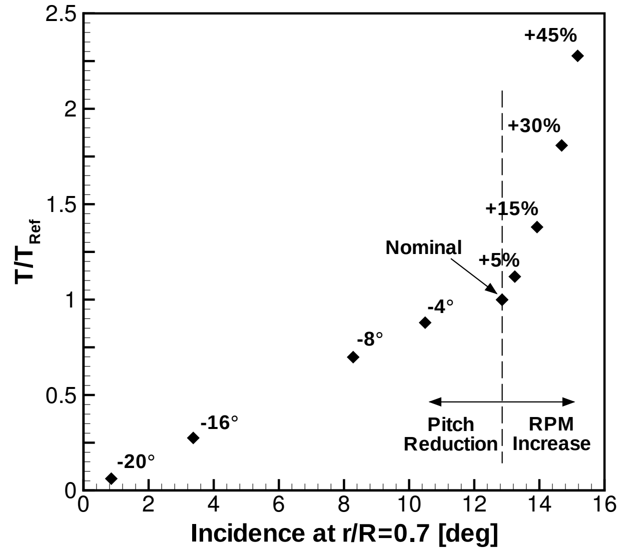

(a) Thrust versus incidence

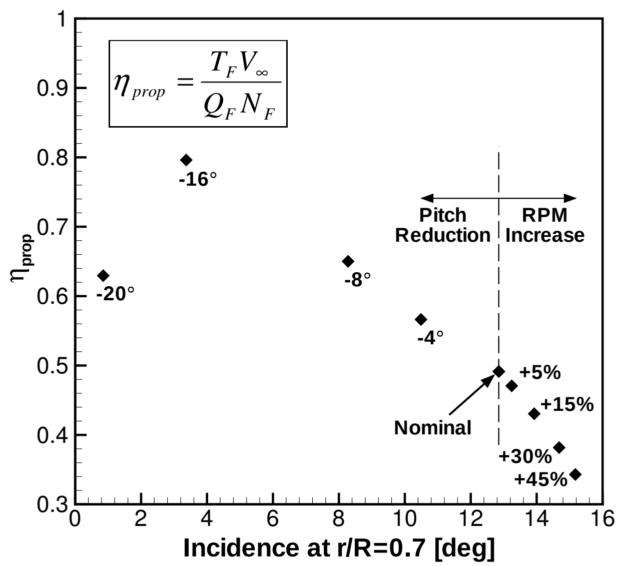

(b) Propeller efficiency versus incidence

Figure 10: Performance trade-offs due to rotor re-pitch and rotational speed increase.

With the effect of pitch and rotational speed separately established, CFD calculations were run at four conditions in which these parameters were combined. A summary of the operating points is given in Table 2. All presented calculations are converged and yield the same rotor thrust to within one percent of the nominal level.

Test Case	ΔN_F (%)	*Incidence at r/R =0.7*	$M_{rel,tip}$	η_{prop}
Nominal	0	12.8°	0.591	0.49
Re-Pitch -4°	+5	10.8°	0.618	0.54
Re-Pitch -8°	+12	9.3°	0.655	0.58
Re-Pitch -16°	+34	6.4°	0.772	0.66
Re-Pitch -20°	+50	5.2°	0.856	0.68

Table 2. Front rotor takeoff operating conditions with combined re-pitch and increased rotational speed.

The tip flow structure as a function of combined re-pitch and speed up are compared in Fig. 11 by means of contours of entropy function. As more re-pitch and speed up are applied, the incidence drops continuously to the case where the rotor pitch is reduced by 20°. At this condition the speed is increased by 50 percent relative to nominal. This results in a significantly reduced size of the tip flow structure.

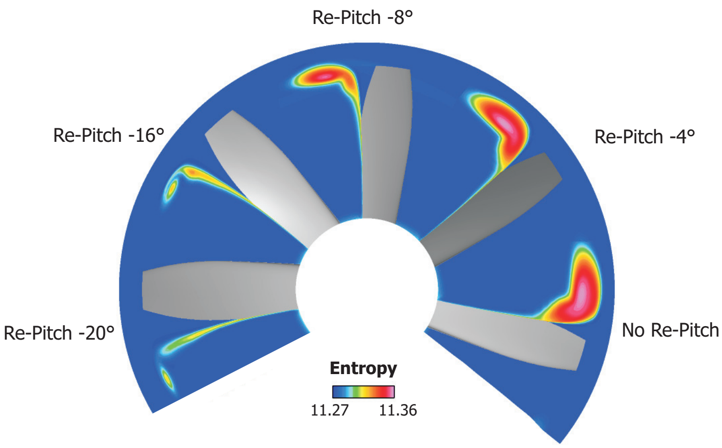

Fig 11. Contours of entropy function downstream of the front rotor due to combined blade re-pitch and speed up.

Figure 12 compares the limiting streamlines on the blade suction surface. The streamlines show that by reducing the rotor incidence, the leading edge vortex can be controlled. As the pitch angle is reduced, the radial location at which the leading edge flow starts to separate moves up the span. At "Re-Pitch -20°", the leading edge vortex has been totally eliminated owing to an incidence distribution comparable to cruise. At these low incidences, the flow exhibits a two-dimensional pattern except at the tip.

The downside of increasing the tip speed is that the relative Mach numbers increase (Table 2) causing the leading edge separation mechanism to change from being incidence driven to shock driven. At the tip, the relative Mach number increases from 0.59 for the nominal takeoff operating point to 0.86 for a highly re-pitched case. The higher Mach numbers give rise to a region of supersonic flow near the blade leading edge terminated by a shock which creates a separation bubble as a result of shock-boundary layer interaction. The location of the separation bubble is illustrated in red for the "Re-Pitch -20°" case.

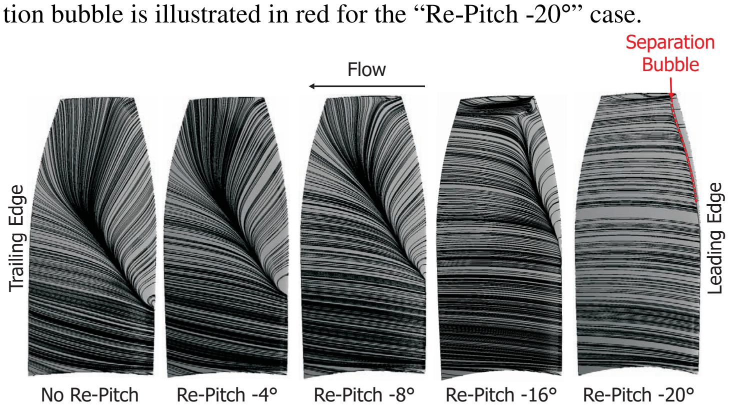

Fig. 12. Effect of re-pitching and speeding up on the rotor suction surface limiting streamlines at takeoff.

Radial distributions of stagnation pressure loss coefficient are compared in Fig. 13. The main benefit of an improved operation on the aerodynamics is that the tip losses are greatly reduced. At the hub, a separation that is also visible in Fig. 12 reduces as the incidence is dropped because the blade root sections are unloaded, reducing the cross-flow pressure gradient. The wake loss across much of the span increases slightly as a result of a loading redistribution. Note that the propeller efficiency increases from 49% for the nominal condition to 68% for a highly re-pitched condition (Table 2).

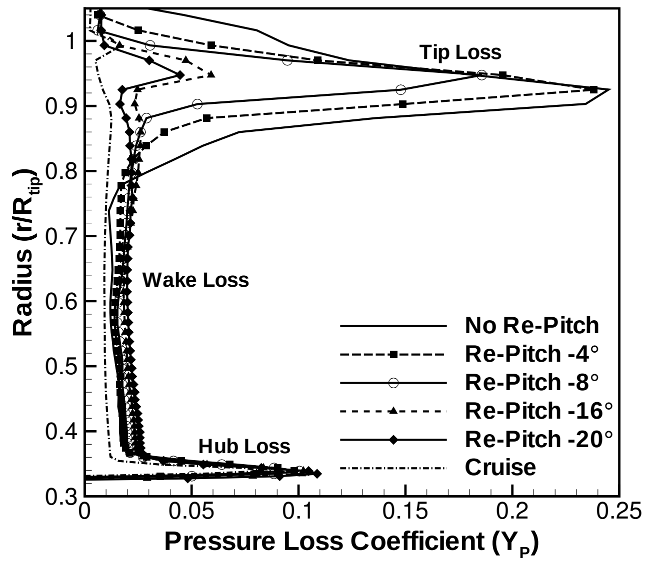

Fig 13. Radial distribution of front rotor stagnation pressure loss coefficient (Y_P) due to operating point variation at takeoff.

As the rotor is re-pitched and sped up, the torque is found to reduce for a given thrust. While the front rotor, in a re-pitched and sped up configuration, generates the same thrust as for the nominal condition, the rear rotor operating point (both pitch and speed) would also have to be adjusted in order for the engine to generate the same total thrust. There could therefore be small changes to the front rotor aerodynamics as a result of the rear rotor. However, the trends shown by these results should not be affected.

Figure 14 tracks the path of the front rotor tip vortex core downstream of the front rotor, as calculated by CFD. The path is traced using an Eigenmode analysis in which the real components of the eigen-analysis of the velocity gradient tensor are used to determine the axes of swirl [25, 26]. The data on the figure shows that reducing the rotor torque reduces the streamtube contraction downstream of the rotor. In the figure, the front rotor pitch change axis is located at x/D = -0.02. Although the influence of the rear rotor on the front rotor flow-field is neglected in this study, the calculations indicate that the streamtube contraction reduces due to the improved operation, an effect which should not be modified by the rear rotor captured streamtube. In this case, at the axial location where the rear rotor PCA would be, x/D = 0.21, the streamtube contracts by 9.7 percent in terms of rotor tip radius for the nominal condition. For the "Re-Pitch -20°" condition, the streamtube only contracts by 7.1 percent. The CFD calculations show the potential to reduce streamtube contraction downstream of the front rotor which, for a well-designed and operated contra-rotating open rotor, could help reduce the amount of cropping used on the rear rotor to avoid tip vortex interaction. In turn, less cropping would minimise the efficiency lost due to residual swirl left in the flow due to the shorter rear rotor.

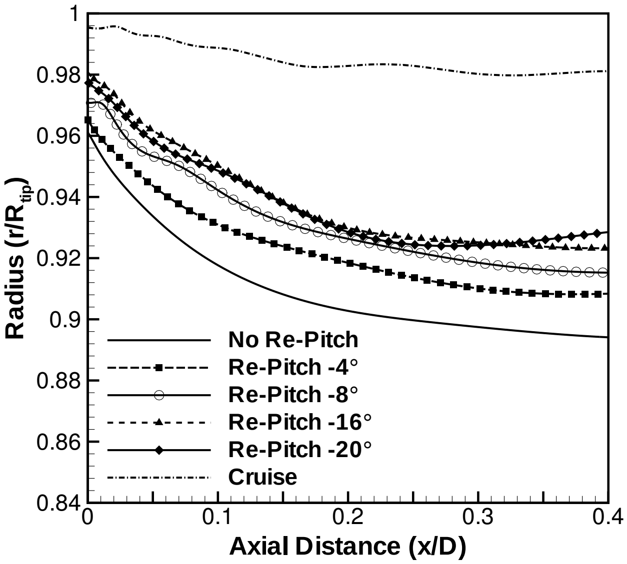

Fig. 14. Calculated front rotor tip vortex contraction due to operating point variation at takeoff.

Figure 15 compares the wake shapes at 70% radius on an axial cut plane located at 0.05 hub chords downstream of the rotor hub trailing edge. For a given momentum deficit, a narrow wake with a large centreline velocity deficit is generally more detrimental with respect to noise than a wake which has a more sinusoidal shape over the blade passage. A wider wake with a smaller velocity deficit reduces the high frequency harmonic content and produces less noise at lower frequencies. Between the nominal and "Re-Pitch -20°" cases, the velocity deficit at the wake centreline reduces by approximately 8 % and the wake-width is 3 times larger. This is achieved by reducing the sectional drag and through additional wake mixing between where the wake was generated and the traverse location.

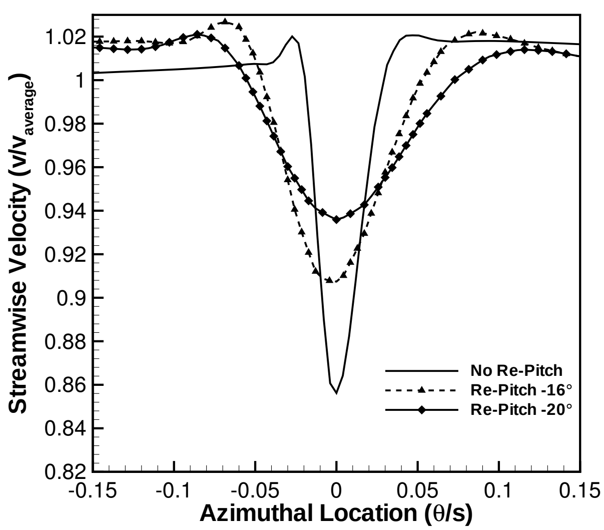

Fig 15. Wake profiles at r/R = 0.70 downstream of the front rotor trailing edge.

EFFECT OF OPERATING POINT ON NOISE

This section explores the potential noise reduction benefits of the improved operation at takeoff. In the previous section it was possible to use CFD results for a single rotor. However, the effect of the rear rotor response to the front rotor flow disturbances is essential to the noise assessment and therefore the rear rotor was included in the noise prediction scheme using a consistent operating point. This can be specified by assuming the contra-rotating rotors are driven through an epicyclic gearbox with a fixed torque split. In this study an equal torque split was applied. The condition at which the rear rotor operates was then determined by applying constant front rotor thrust and constant total thrust as constraints.

Noise predictions were obtained using CRPFAN [14] for each of the operating conditions given in Table 2. In each case, the CFD results from the front rotor were used to set the spanwise distributions of lift and drag coefficients input to the noise prediction. The chordwise loading distributions in the predictions were selected as those giving the best agreement with rig data. In addition, the streamtube contractions predicted in the CFD calculations were used to specify the radial location of the interaction between the front rotor tip vortex and the rear rotor.

The predicted noise results are presented as directivity plots of rotor-alone, rotor-rotor interaction and dBA sound pressure levels (SPL) at an arc of constant radius, as illustrated in Fig. 16. The origin is assumed to be halfway between the rotor pitch change axes.

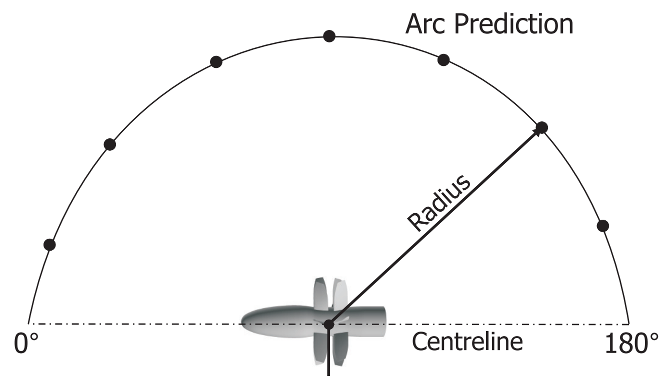

Fig. 16. Orientation of noise prediction locations.

The front and rear rotor-alone tones at 1 and 2 BPF (blade passing frequency) are given in Fig. 17. As expected, increasing the front rotor rotational speed raises the noise levels near the rotor plane of rotation with an effect more pronounced at 2 BPF. The increase of rear rotor noise results from the increase in its rotational speed to satisfy the constant torque split. For the "Re-Pitch -4°" and "Re-Pitch -8°" cases, the plot shows lower noise levels than the nominal condition. This is because the equal torque split requires a lower rotational speed than for the "No Re-Pitch" case and therefore the peak noise reduces at a given thrust.

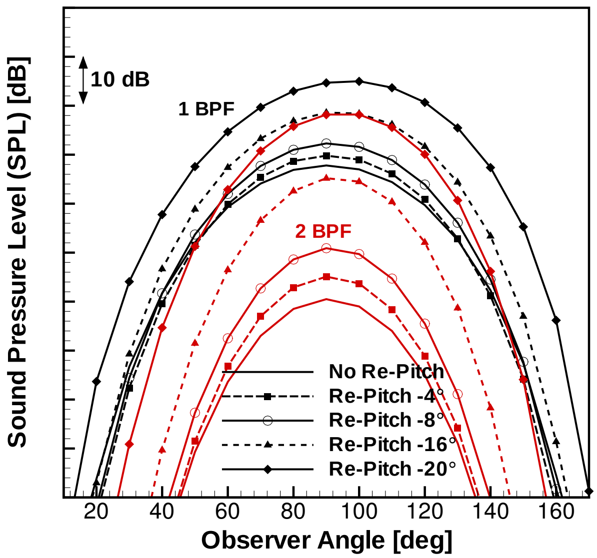

(a) Front rotor

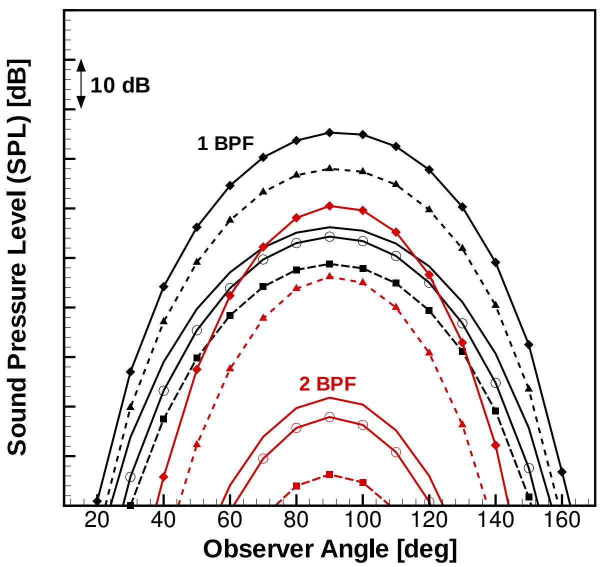

(b) Rear rotor

Fig. 17. Comparison of the predicted front and rear rotor-alone tones at 1 and 2 BPF.

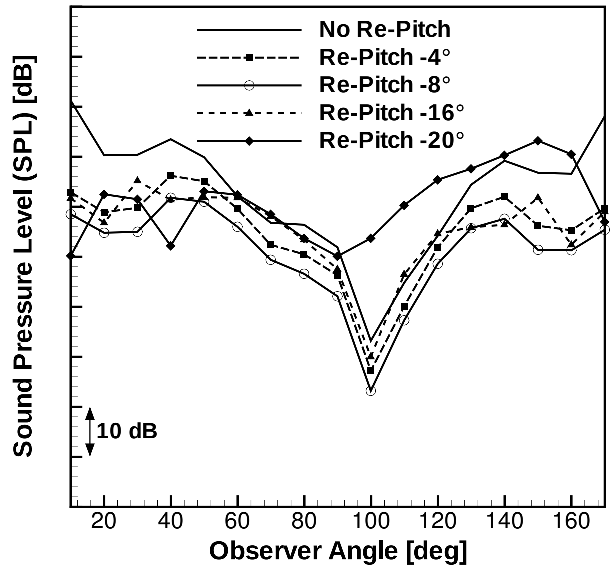

(a) (1,1) interaction tones

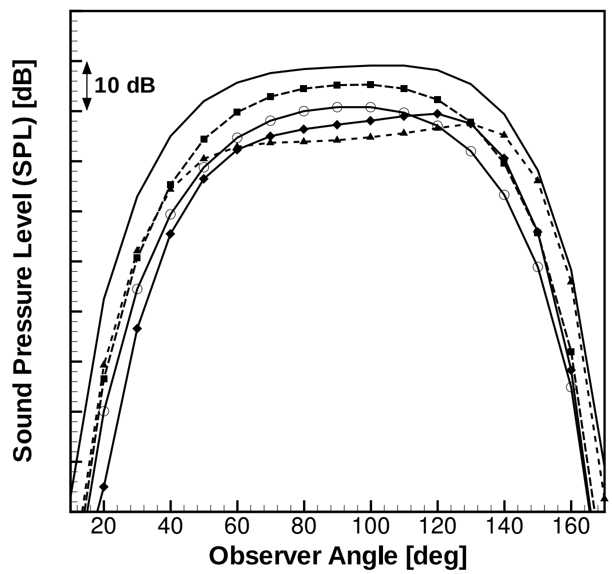

(b) (1,2) interaction tones

Fig 18. Comparison of the predicted (1,1) and (1,2) interaction tones.

The directivity plots for the (1,1) and (1,2) rotor-rotor interaction tones are presented in Fig. 18. In general, the predicted radiated noise reduces in line with the reductions in the magnitude of the front rotor wake caused by re-pitching (Fig. 15). Differences of up to 7 dB are predicted for an observer location in a plane between the two rotors. However, for highly re-pitched and sped up cases the interaction SPL increases. In the “Re-Pitch -20°” case the noise increases significantly in the rear arc owing to the interaction between a fast spinning rear rotor and the wakes from the front rotor.

Note that for the (1,1) interaction tone, a dip is created in the vicinity of the plane of rotation because $B_F = B_R$ on Rig-140. This leads to a plane wave mode which peaks on the rig centreline.

To answer how Rig-140 should be operated for minimum noise at takeoff, the dBA SPL has been calculated for each case considered. The reductions in terms of dBA SPL are shown in Fig. 19 relative to the nominal condition. As the operating point changes, the results indicate that significant noise reductions can be achieved.

The predicted noise reductions are mainly the result of the diminishing contribution of interaction tones to the total noise in the forward and rear arcs. Near the planes of rotor rotation, the total noise is found to protrude relative to the nominal condition for the highly re-pitched case, “Re-Pitch -20°”, owing to the high tip speeds at which the rotors operate. This partly increases rotor-alone noise but also increases interaction noise as the wake and tip vortex structures change and interact with a faster spinning rear rotor.

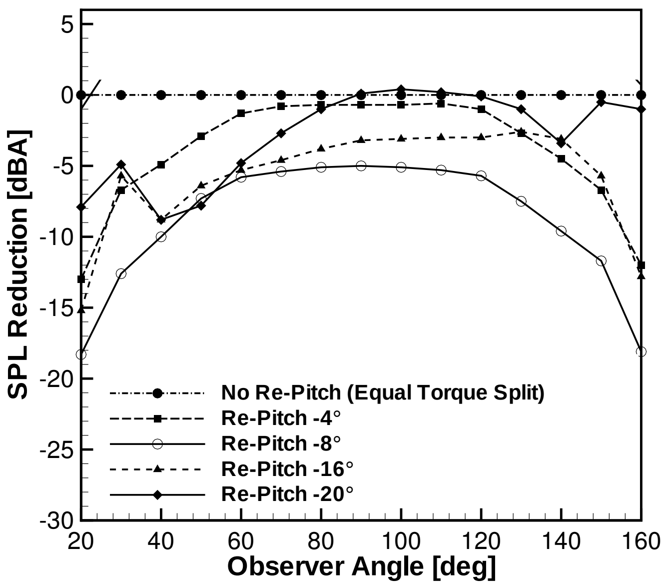

Fig. 19. Predicted sound pressure level (dBA) reduction relative to the nominal condition at takeoff.

For minimum noise, the CRPFAN method suggests that the front rotor of Rig-140 should be operated with an 8° re-pitch from nominal at takeoff. At this condition, the radiated noise reduces significantly relative to the nominal condition at all observer angles with reductions of the order of -18 dBA at the extremes of the directivity.

RELEVANCE TO CURRENT DESIGNS

The design of contra-rotating open rotors has developed significantly since the testing of Rig-140. Current designs generally feature highly swept front and rear rotors with novel spanwise variations of twist, chord and camber. The blade counts of the front and rear rotors are different and chosen to control the blade loading and noise characteristics. Rear rotor crop is often used to reduce tip vortex interaction and, unlike Rig-140, the rear rotor design is usually quite distinct from the front rotor. In addition, the torque split between the front and rear rotor can be different.

The introduction of sweep to an open rotor blade has various beneficial effects. Firstly, at cruise, sweep reduces relative Mach numbers and thus reduces losses associated with shock waves [27]. At takeoff, relative Mach numbers will also be reduced, but the sweep will also affect the formation and trajectory of the leading edge vortex. In general, for a given operating point, a swept blade is likely to produce less loss at the tip. In this case, the amount of re-pitch and speed up needed to clean up the flow on the front rotor would be reduced. However, some adjustment of the operating point will still be beneficial as it would also improve the front rotor wake profiles, as shown in Fig. 15.

Rotor designs with improved chord, camber and twist distributions should operate at lower incidence at takeoff, relative to Rig-140, and have an improved spanwise incidence variation. However, the non-dimensional blade lift is a lot higher at takeoff than at cruise for all designs and therefore the front rotor wakes and losses will still be significant. Some re-pitch and speed up should enable improvement to the aerodynamics and noise and if this is not the case, it is likely that the rotor performance at cruise will have been compromised.

For open rotor configurations with different blade counts, the approach of re-pitching and speeding up the front rotor is still applicable. For a given thrust, the blades of a higher solidity rotor would operate at lower incidence than in the case of Rig-140. Therefore, the pitch reduction and the associated increase in rotor speed required to achieve better aerodynamics would be less extreme. Similarly, a different torque split introduces another degree of freedom to a design, which could enable lower incidence levels at takeoff and reduced re-pitch requirements. However, it is important to note that the torque-split is fixed for any given design and the approach of re-pitching and speeding up the front rotor is still applicable, provided the rear rotor is operated appropriately to compensate the varying front rotor torque.

Other work in the literature illustrates that the effects of changes in blade speed for a fixed geometry are particularly applicable to modern open rotors. For example, Parry and Vianello [28] started with the same Rig-140 configuration used here and conducted a detailed parametric study of changes in front and rear blade numbers, as well as simultaneous changes in front and rear blade speeds, to improve the noise at takeoff conditions. Their study, though, was based on a lower fidelity (public domain) aerodynamic calculation [29] than the CFD used here. In addition, the authors note the recent patent of Parry *et al.* [30] which refers specifically to noise reduction on modern open rotors for designs which combine particular blade numbers together with operating the rotors at higher tip rotational speeds at takeoff than at the cruise design point.

CONCLUSIONS

At the nominal takeoff condition of Rig-140, high front rotor incidence causes the flow to separate at the blade leading edge and roll-up into a leading edge vortex. This is convected towards the tip where it combines with the tip vortex, leading to a major source of loss downstream of the front rotor. This loss core moves radially inwards due to streamtube contraction and interacts with the rear rotor tip flow.

Mitigating the front rotor leading edge separation is key to improving the open rotor performance at takeoff. The high incidence at which the rotor operates is the root cause of the problem leading to large losses and high rotor-rotor interaction noise. By re-pitching the front rotor and increasing its rotational speed, the incidence can be reduced to levels more typical of cruise operation. The leading edge vortex flow is diminished and the flow downstream of the front rotor becomes much cleaner, with a concentrated viscous wake and tip vortex. For Rig-140, the front rotor propeller efficiency increases from 49% to 68% for highly re-pitched and sped up cases. The change in operating condition also slightly reduces the streamtube contraction between the rotors.

Noise predictions show that the diminished wake caused by the change in front rotor operation leads to significantly lower viscous wake interaction noise. However, rotor alone noise increases slightly due to higher rotational speeds. The results indicate that through careful operation, with moderate levels of re-pitch and speed increase, the noise of an open rotor can be significantly reduced across all directivities.

The findings in this paper are applicable to any open rotor design in which the non-dimensional lift at takeoff is high due to insufficient rotational speed. In advanced designs that are highly swept with differing blade counts, rear rotor crop and different rotor torque splits the quantitative effects of re-pitching and speed up are likely to be different from Rig-140. However, there will always be scope to improve open rotor aerodynamics and noise via the mechanisms demonstrated in the current study.

ACKNOWLEDGEMENTS

The authors would like to thank Rolls-Royce plc and the EPSRC for funding and supporting this work. The authors are particularly grateful to Rolls-Royce for granting the permission to publish this paper.

REFERENCES

[1] Smith, L. H., Jr., 1987, "Unducted Fan Aerodynamic Design", ASME J. Turbomach., **109**(3), pp. 313-324.

[2] Hager, R. D. and Vrabel, D., 1988, "Advanced Turboprop Project", NASA SP-495.

[3] Mitchell, G. A., 1988, "Experimental Aerodynamic Performance of Advanced 40°-Swept, 10-Blade Propeller Model at Mach 0.6 to 0.85", NASA TM-88969.

[4] Neumann, H. E., Bober, L. J., Serafini, J. S. and Chang, L.-K., 1983, "An Analytical and Experimental Comparison of the Flow Field of an Advanced Swept Turboprop", AIAA-1983-189.

[5] Podboy, G. G. and Krupar, M. J., 1989, "Laser Velocimeter Measurements of the Flow Field Generated by an Advanced Counterrotating Propeller", AIAA-1989-434.

[6] Shin, H.-W., Whitfield, C. E. and Wisler, D. C., 1994, "Rotor-Rotor Interaction for Counter-Rotating Fans, Part 1: Three-Dimensional Flowfield Measurements", AIAA J., **32**(11), pp. 2224-2233.

[7] Celestina, M. L., Mulac, R. A. and Adamczyk, J. J., 1986, "A Numerical Simulation of the Inviscid Flow through a Counter-Rotating Propeller", ASME Paper 86-GT-138.

[8] Schnell, R., Yin, Y., Voss1, C., Nicke1, E., 2010, "Assessment And Optimization of the Aerodynamic And Acoustic Characteristics of a Counter Rotating Open Rotor", ASME Paper GT2010-22076.

[9] Peters, A. and Spakovszky, Z.S., 2010, "Rotor Interaction Noise in Counter-Rotating Propfan Propulsion Systems", ASME Paper GT2010-22554.

[10] Zachariadis, A. and Hall, C. A., 2009, "Application of a Navier-Stokes Solver to the Study of Open Rotor Aerodynamics", ASME Paper GT2009-59332.

[11] Kirker, T. J., 1990, "Procurement and Testing of a 1/5 Scale Advanced Counter Rotating Propfan Model", AIAA-1990-3975.

[12] Moinier, P. and Giles, M. B., 1998. "Preconditioned Euler and Navier-Stokes Calculations on Unstructured Grids". In 6th ICFD Conference on Numerical Methods for Fluid Dynamics, Oxford, UK.

[13] Spalart, P. R. and Allmaras, S. R., 1994 "A One-Equation Turbulence Model for Aerodynamic Flows", La Recherche Aerospatiale, **1**, pp.5-21.

[14] Whitfield, C. E., Mani, R., and Gliebe, P. R., 1990, "High Speed Turboprop Acoustic Study (Counterrotation), Volume II, Computer Programs". Technical Report, NASA CR-185242.

[15] Whitfield, C. E., Mani, R., and Gliebe, P. R., 1990, "High Speed Turboprop Acoustic Study (Counterrotation), Volume I, Model Development". Technical Report, NASA CR-185241.

[16] Hanson, D. B., 1980, "Helicoidal Surface Theory for Harmonic Noise of Propellers in the Far Field", AIAA J., **18**(10), pp 1213–1219.

[17] Majjigi, R. K. and Gliebe, P. R., 1984, "Development of a Rotor Wake/Vortex Model", Volume I, Final Technical Report. NASA CR-174849.

[18] Majjigi, R. K., Uenishi, K., and Gliebe, P. R., 1989, "An Investigation of Counter-rotating Tip Vortex Interaction". NASA CR-185135.

[19] Sears, W. R., 1941, "Some Aspects of Non-Stationary Airfoil Theory and Its Practical Application", J. Aeronaut Sci, **8**(3), pp 104–108.

[20] Amiet, R. K., 1976, "High Frequency Thin-Airfoil Theory for Subsonic Flow", AIAA J., **14**(8), pp 1076–1082.

[21] Cumpsty, N. A., 1977, "A Critical Review of Turbomachinery Noise". ASME J. Fluids Engineering, **99**, pp 278–293.

[22] Parry, A. B. and Crighton, D. G., 1989, "Prediction of counter-rotation propeller noise", AIAA Paper 1989-1141.

[23] Parry, A. B., 1997 "Modular prediction scheme for blade row interaction noise", J. Propulsion Power **13**, 334-341.

[24] Vaczy, C. M. and McCormick, D. C., 1987, "A Study of the Leading Edge Vortex and Tip Vortex on Prop-Fan Blades," ASME J. Turbomach., **109**(3), pp. 325-331.

[25] Sujuki, D. and Haimes, R., 1995, "Identification of Swirling Flow in 3-D Vector Fields", AIAA-1995-1715.

[26] Haimes, R. and Kenwright, D., 1999, "On the Velocity Gradient Tensor and Fluid Feature Extraction", AIAA-1999-3288.

[27] Metzger, F. B. and Rohrbach, C., 1986, "Benefits of Blade Sweep for Advanced Turboprops", J. Propulsion, **2**(6), pp. 534-540

[28] Parry, A. B. and Vianello, S., 2010 "A Project Study of Open Rotor Noise", presented at the 14th CEAS-ASC Workshop (& 5th Scientific Workshop of X3-Noise), Warsaw, Poland, 7-8 Oct.

[29] Maksymiuk, C. M. and Watson, S. A., 1983 "A computer program for estimating the aerodynamic characteristics of NACA 16-series airfoils", NASA Tech. Memo 85696.

[30] Parry, A. B., Howarth, N. and Taylor, M. D., 2008, "Aeroengine", International Publication No. WO 2008/096124 A2.